Beam Test Results of the LHCb Electromagnetic Calorimeter.

LHCb Public Note

Issue: 1
Revision: 0

Reference: LHCb 2007-149
Created: December 17, 2007
Last modified: April 7, 2008

Prepared by: A. Arefiev[a], S. Barsuk[b], I. Belyaev[a], B. Bobchenko[a], L. Camilleri,[c] V. Egorychev[a], Yu. Gilitsky[d] A. Golutvin[a], O. Gouchtchine[a], I. Korolko[a], T. Kvaratskheliya[a], I. Machikhilian[a], M. Martemianov[a], E. Melnikov[a], A. Morozov[a], M. Prokudin[a], D. Roussinov[a], V. Rusinov[a], A. Schopper[c], S. Schuvalov[e], A. Soldatov[d], E. Tarkovski[a], K. Voronchev[a]

[a]Institute for Theoretical and Experimental Physics, B. Cheremushkinskaya, 25, Moscow 117259, Russia

[b]Laboratoire de l'Accelerateur Lineaire, Universite Paris-Sud 11, Bat 200, 91898 Orsay cedex

[c]European Organization for Nuclear Research, CERN, CH-1211, Geneve 23, Switzerland

[d]Institute of High Energy Physics, Protvino Moscow region, 142248, Russia

[e]Deutsches Electronen Synchrotron, Platanenallee 6 D-15738 Zeuthen

Abstract

The main properties of the LHCb electromagnetic calorimeter and a prototype of the monitoring system was studied at the X7 CERN test-beam facility. A dedicated MC simulation for light propagation in the scintillator tiles was developed and tuned with experimental data.

Document Status Sheet

1. Document Title: Beam Test Results of the LHCb Electromagnetic Calorimeter.			
2. Document Reference Number: LHCb 2007-149			
3. Issue	4. Revision	5. Date	6. Reason for change
Draft	1	January 24, 2008	Second version. Checked by referee

Contents

List of Figures

List of Tables

1 Introduction

During the last 25 years sampling calorimeters of "shashlik" type have proven their applicability for a wide range of high energy physics experiments. This type of calorimeter was successfully operated at PHENIX [1] at BNL, DELPHI [2] at CERN and HERA-B [3] at DESY. Wave length shifting (WLS) fibers used for the scintillator light readout allow us to build hermetic calorimeters with minimal amount of dead material. Fast response, adequate energy resolution, radiation resistance, flexible transverse and longitudinal granularity of these detectors and a relatively moderate cost make them very attractive to use in large modern experiments.

Since the first large scale "shashlik" electromagnetic calorimeter built for the PHENIX detector a lot of efforts were done to improve the quality of the scintillator plates and to develop facilities for their mass production. Work was aimed mainly at improving the uniformity of detector response, especially at the tile edges. Early "shashlik" modules were built with transparent edges of the plastic plates. Later physicists developed scintillator plates with mirrored edges, which improved the overall light collection efficiency. However, mirroring is not able to compensate for the decrease of detector response at the outer border of the modules, which is caused by energy losses in 0.1-0.2 mm of dead material in between the modules. For the LHCb electromagnetic calorimeter (henceforth referenced as ECAL) we have used another technology for covering the plastic tile edges with special chemicals to ensure diffuse reflection of the scintillating light, resulting in an increase of light collection close to the tile edges. This technique helps to compensate for dead material effects.

At the same time a lot of efforts were devoted to the development of a reliable, robust and cheap monitoring system to control the performance and radiation induced damages of the detector during long (5-10 years) data taking periods at LHC. Precise monitoring of all detector components is very important for future LHC experiments. The LHCb calorimeters [4] provide fast measurements used already at the level_0 trigger for selecting events with high E_T decay products of B mesons. Fast on-line monitoring of the ECAL performance is crucial for the uniformity of trigger selection over the whole calorimeter area. Monitoring is also important for the off-line data analysis providing the possibility to eliminate the variations in detector response caused by power supply and temperature instabilities.

The electromagnetic calorimeter of the LHCb detector [4] was built taking into account these considerations. In this article we describe the test beam measurements of the LHCb ECAL modules, concentrating on light collection uniformity and performance of the monitoring system prototype. In order to verify our understanding of the ECAL behavior we have developed a dedicated Monte Carlo program to simulate the light propagation in different scintillator tiles. The parameters of this program were tuned using experimental data from beam tests. The Monte Carlo simulation is able to reproduce all measured effects.

2 Test-beam setup

Experimental studies of the LHCb electromagnetic calorimeter modules were performed at the X7 beam, which is a part of the West Area test beam complex at CERN. The detailed drawing of the optics of the X7 beam, indicating the positions of all magnets, collimators and detectors is presented in Figure 1 [5]. The beam momentum settings were used in the range between 5 and 100 GeV/c. The beam polarity was negative, and particles available were π^-, e^- and μ^-. The electron beam was produced using a lead sheet to convert photons from neutral pion decays, while the muon beam used a beam dump to absorb all secondary particles except muons.

The beam was operated in a slow spill mode of 4 seconds duration repeated every 17 seconds. An instantaneous particle rate was normally restricted to a few thousand particles per second. Beam profiles are determined using the collimator settings. For light collection uniformity studies we have used a rather wide beam with a width of 30 mm horizontally and 30 mm vertically. The energy resolution was measured with a decreased slit in the horizontal collimator to minimize the momentum spread of electron beam down to $\sim$1.0%.

All three types of the LHCb ECAL modules with different cell sizes, shown in Figure 2 were tested. A module stack is built from alternating layers of 2 mm thick lead, white reflecting 120 μm thick TYVEK

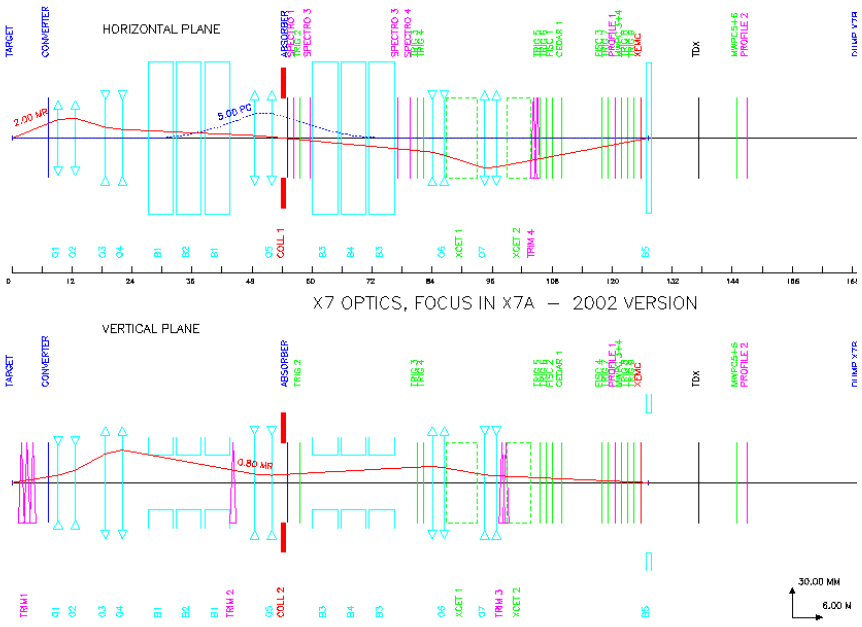

Figure 1 General layout of the X7 beam area at CERN.

paper (DuPont Tyvek®) and 4 mm thick scintillator tiles (Figure 2, right). In depth, the 66 Pb and scintillator layers form a 42 cm stack corresponding to a radiation length of 25 X_0. The stack is wrapped with black paper to ensure light tightness. It then is compressed and fixed from the sides by welding 100 μm steel tapes. The light from the scintillator tiles is transported by 1.2 mm diameter wavelength shifting (WLS) fibers that penetrate the entire module, and is then read out with a photomultiplier tube (PMT). A quadrangular prism light mixer made from polystyrene is inserted between the end of the fiber bundle and the PMT. Through the center of each cell a clear fiber transports light from a dedicated monitoring system to the PMT at the rear of the module. All tested modules were equipped with the standard LHCb calorimeter photomultipliers (PMT) of type Hamamatsu R7899-20. The high voltage is generated using a Cockcroft-Walton (CW) base. On the printed circuit boards of the CW base a clipping line performs the shaping of the PMT pulse in order to eliminate a small tail extending after 25 ns readout interval. The shaped signals were readout using LeCroy 2249W (12 bits) ADCs with 70 ns gate.

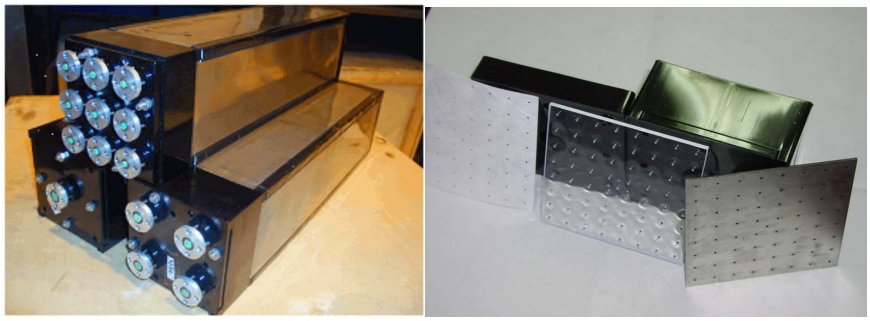

Figure 2 *Left:* Outer, middle and inner type modules; *Right:* Scintillator tile, lead plate and TYVEK paper compounds of the stack. Also shown are the housings for fiber loops on the front of the module and fiber bundles on the rear of the module.

The beam line was instrumented with scintillation counters to form the beam trigger. Three sets of delay wire chambers [6] with a typical spatial resolution of 0.2 mm were used to reconstruct the beam particle trajectory and to determine the particle entry point at the calorimeter module surface. The

arrangement of the tested calorimeter modules and delay wire chambers at the beam line is shown in Figure 3.

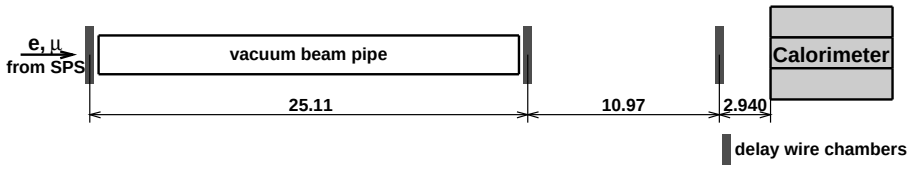

Figure 3 Sketch of the LHCb calorimeter test beam installation.

The last delay wire chamber (closest to the calorimeter) was used only in 2004 during beam tests of the inner calorimeter modules to improve the precision of the tracking system, reducing multiple scattering effects and eliminating incorrectly measured tracks. Tracks were fitted with a straight line in both (X and Y) projections. For further analysis we used only good quality tracks requiring the χ^2 fit to be less than 4. The precision and efficiency of the tracking is demonstrated in Figure 4 where we plot the distance between the actual coordinate measured using the last delay chamber, and the intersection of the fitted track with the chamber plane. About 45% of tracks are selected with this procedure. The RMS of the distribution corresponds to 0.2 mm spatial resolution of the delay wire chambers convoluted with 0.165 mm additional contribution due to the multiple scattering in the air.

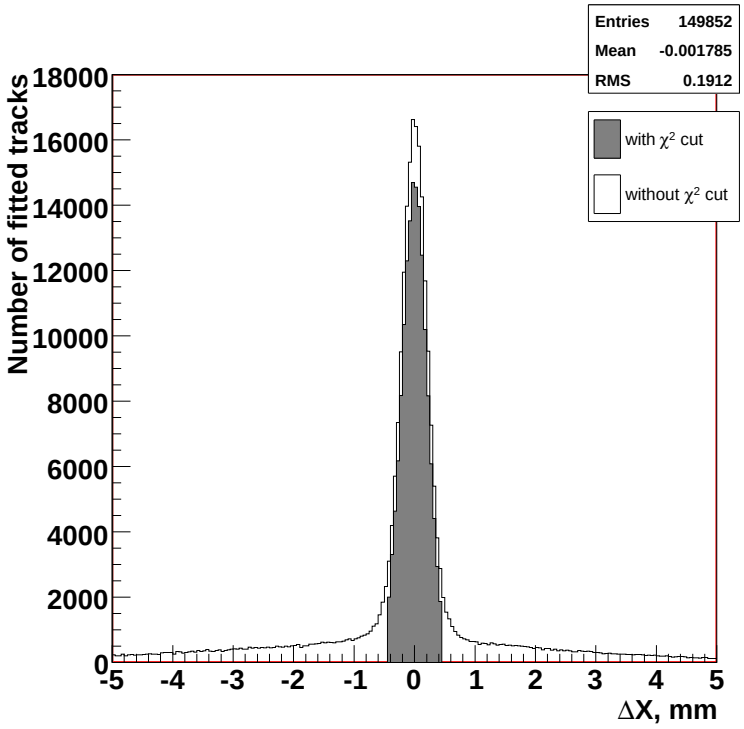

Figure 4 Precision of test beam tracking system.

The calorimeter modules were positioned onto a motorized rotating table which is moving both in the horizontal and vertical directions. During the module scan the table movements could be controlled using a dedicated PC with a precision of about 2 mm, which is not sufficient for our experimental needs. In order to improve the position accuracy we have developed a special algorithm based on the perfect collinearity of fibers with the beam direction. A small fraction (about 1%) of incoming particles hits fibers and therefore deposits less energy in the module. Selecting such rare particles we were able to measure the position of the fibers as shown in Figure 5 for a each position of the moving table, during a muon scan of the inner module. Several fibers (WLS or clear monitoring fiber) can be seen

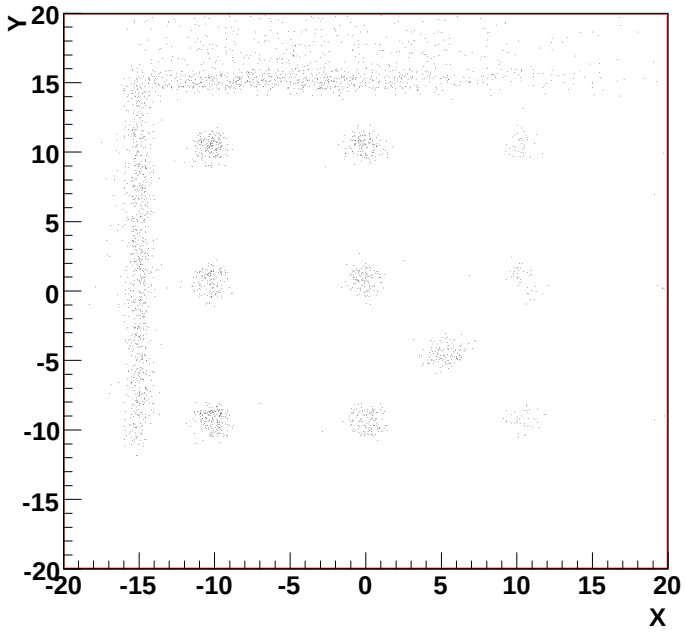

Figure 5 Fibers seen in the cell of the inner module for a given moving table position.

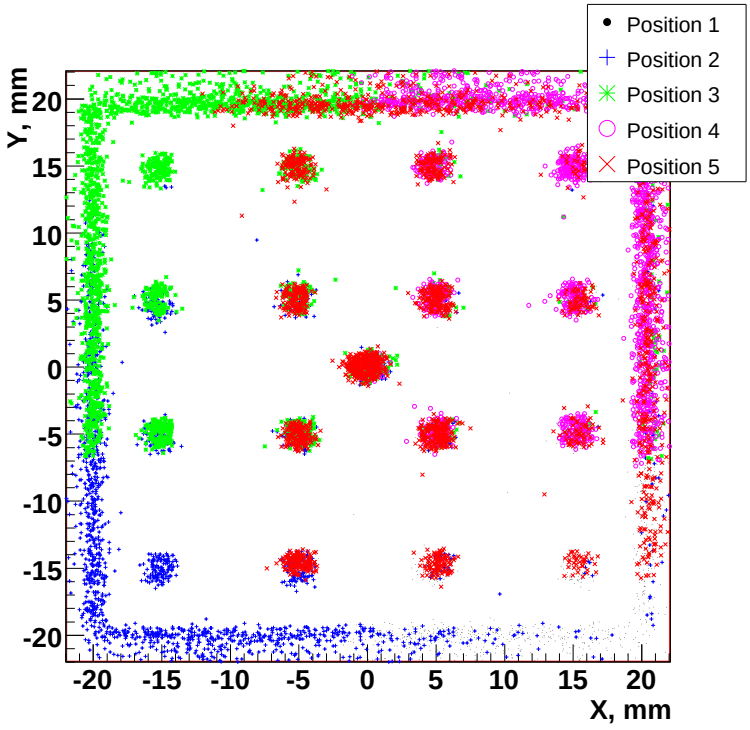

Figure 6 Image of all fibers of the LHCb inner module, using the procedure described in the text.

simultaneously in subsequent positions of the moving table. By requiring the measured coordinates of these fibers to be the same and the clear fiber to be located at the (0,0) point, a common reference system has been defined, as shown in Figure 6. The complete structure of the LHCb inner module cell is clearly seen. The precision in positioning the fibers was estimated to be better than 0.15 mm. A similar method was also used for the electron scan.

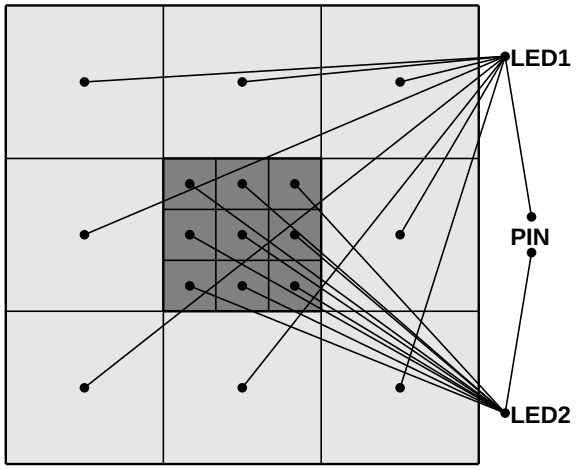

Figure 7 Sketch of the monitoring system used for the test of the inner LHCb calorimeter module.

The test beam setup of the calorimeter modules was equipped with a prototype of the monitoring system of the LHCb ECAL detector.This allowed us to test all components of the monitoring system and to guarantee the required precision of about 0.2% over the 1-2 days long measurement of the uniformity of light collection efficiency and the detailed studies of energy resolution. The monitoring system is based on light-emitting diodes (LEDs), controlled with Hamamatsu S223-01 PIN photodiode (henceforth simply referenced to as PIN) that is illuminated with light carried in separate optical fiber channels directly from LEDs, as shown schematically in Figure 7. Two LEDs were fired with dedicated LED drivers triggered using an external generator operated at 1500 Hz frequency. Every first and third generator pulse triggered one LED, second and forth pulses triggered another LED. Every fifth pulse was used to store an empty event for permanent control for the position and width of pedestals.

The ECAL monitoring system prototype was implemented and extensively tested in 2002/2004 beam tests at CERN. One of the aims of these tests was to demonstrate the ability of the proposed system to monitor gain drifts in the photomultiplier tubes to the required precision. Experimental conditions at the X7 beam area with significant diurnal temperature variation ($\sim$10 degrees per day) gave an outstanding opportunity for such tests. The response of the calorimeter module to the 50 GeV electrons was measured during almost 24 hours (one 5 minutes run per every 30 minutes). The response of this module to LED flashes with $\sim$600 Hz rate was measured at the same time and controlled independently using a PIN diode. The typical raw electron signal averaged over one run is shown in Figure 8. The large width of the distribution is explained by the $\sim$1% dispersion of electron momentum and significant transverse dimensions of the beam $\sim 30mm \times 30mm$. The monitoring LED signal mea-

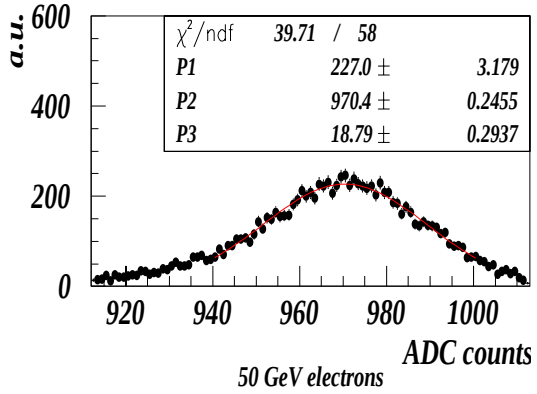

Figure 8 The typical raw electron signal.

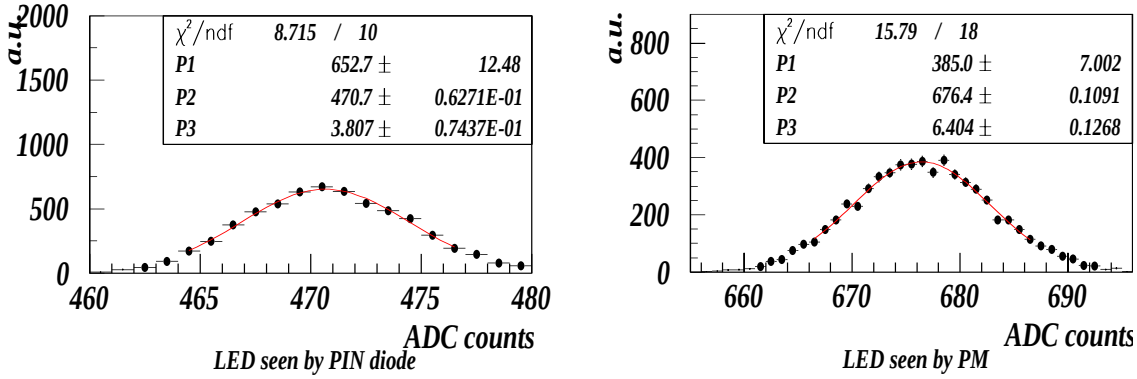

Figure 9 (Left)The LED signal measured by the PIN diode of type Hamamatsu S1223-01. (Right) The LED signal measured by the PMT of type Hamamatsu R7899-20.

sured with the calorimeter photomultiplier and PIN diode during the same run shown in Figure 9 at the right and left respectively. Similar measurements were repeated every 30 minutes.

The variation of the 50 GeV electron and LED signals were measured during 24 hours using the calorimeter photomultiplier and PIN diode responses. The signals, normalized to the initial signal at 0 time, are shown in Figure 10. The raw electron signal amplitude during exposure time has varied by 3%; the variation of the LED flash intensity measured with the PIN diode was even higher, about 6%. The correction factor for the electron signal has been obtained by combining the two independent measurements. The corrected time dependence of the electron signal is shown in Figure 10. The precision of the correction procedure is better than 0.2% which perfectly agrees with the requirements.

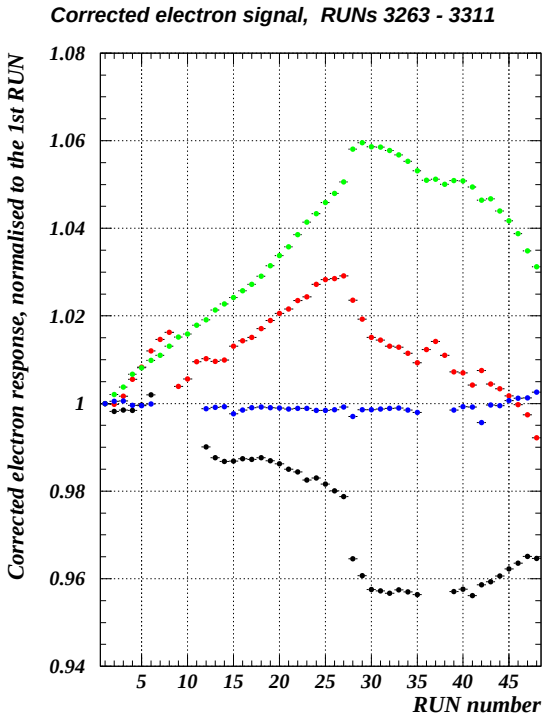

Figure 10 Monitoring system gain correction from test beam data for 22 hours running: green points — LED seen by PIN diode; red points — LED seen by PMT R7899-20; black points — signal from electrons; blue points — signal from electrons corrected on (LED-PIN/LED-PMT) ratio.

3 Light collection simulation

A dedicated ray-tracing program was developed for modeling light collection inside the scintillator cell. Optical processes handled by the ray-tracer involve refraction, mirror and diffuse reflection, attenuation in the medium, and absorption on the plastic surface and in tyvek, which is used to interlay the scintillator and absorber tiles. The reflection and refraction on the transparent tile walls are implemented according to Snell's law [7]. The Fresnel formula for non-polarized light is used for the determination of the reflection and refraction probability on the boundary of two optical mediums. The geometry of the plastic tiles is defined by a set of primitives (cuboid, cone and cylinder) and Boolean operations. A dedicated voxelization procedure is used to speed up calculations. The photon is assumed to propagate along a straight line between two interactions, neglecting diffuse scattering in the scintillator medium.

The geometries of the scintillator tiles correspond exactly to those used for the assembly of the outer, middle and inner modules of the LHCb ECAL. Tiles have cuboid shape with cylindrical holes for the WLS fibers and one clear monitoring fiber in the center of every cell. The edges of the tile are assumed to be coated with special white paint simulating the diffuse reflection due to the chemical treatment described above. To perfectly describe the chemical treatment, the same white paint also covers thin (1.0–1.5 mm) bands around the corners of the tile edge. A scintillator tile with all fibers is covered with tyvek sheets from both sides. Each fiber is modeled by two coaxial cylinders neglecting the double cladding of the WLS fibers used in reality.

In order to compute the map of light collection efficiency the plastic cell is divided in small volumes of $0.5 \times 0.5 \times 4.0\, mm^3$. Photons are generated uniformly inside this volume with isotropic momentum distribution. The photon wave length is generated according to the POPOP emission spectra. Each photon is propagating inside the described setup until:

1. It stops in the scintillator.
2. It is absorbed on the tile surface, in the tyvek, or in the fiber core.

A photon that stopped in the fiber core is re-emitted isotropically with a shifted wavelength corresponding to the WLS fiber re-emission spectrum. The direction of re-emitted photon is then checked to ensure that it is not able to leave the fiber and will reach the photomultiplier window. The small attenuation in the light mixer located between fibers bundle and the PMT is neglected. The computed 2D map of the light collection efficiency is finally convoluted with the measured map of the tile thicknesses, which determines the energy deposition for minimum ionizing particle crossing the tile in a given point perpendicular to its surface. The last step is important because the plastic tile thickness is varying across the tile surface. The result of such convolution is referred later as an effective 2D map of light collection efficiency.

The results of ray-tracing program depend on certain number of parameters such as: photon attenuation length in scintillator, whiteness of tyvek and white paint covering the tile edges, probability of photon absorption on the surface of the plastic tile (so called surface quality) and some others. All these parameters could be extracted from the comparison of simulation results with the experimental measurements of light collection uniformity. Such comparison should take into account the transverse shape of the incoming particle energy deposition in the calorimeter module, which dilutes the intrinsic variation of the light collection. Muon data is therefore most suitable for our purposes. Effective 2D maps of light collection were used in the GEANT [8] program for weighting each elementary energy deposition, depending on the local coordinate in the calorimeter cell. Version 3.21 of GEANT was used, with the tracking carried down to 30 KeV for electromagnetic particles and 30 KeV for hadronic particles. A similar simulation chain was then repeated for electrons with a selected set of effective 2D maps as a cross-check. The algorithms for the reconstruction of the particle energy after the GEANT simulation, correspond exactly to those used in the analysis of the test beam data. The detailed comparison of the experimental data, obtained during the muon and electron scans of the LHCb calorimeter modules, with the simulation results is presented in chapter 4. A tuned set of the ray-tracing program parameters allows us to reproduce the experimental data almost perfectly. Tiny systematic effects (close to the tile borders) are below our experimental precision.

Using the tuned ray-tracing program we have calculated the 2D maps of the light collection efficiency for three different technologies of "shashlik" scintillator tiles production:

Table 1 Comparison of the experimental data and the simulation results on light yield for the three types of the LHCb ECAL modules. The inner module numbers were used for normalization.

	Experimental data	Ray-tracing program
Inner modules	3100	3100
Middle modules	3500	3720
Outer modules	2600	2655

1. tiles with transparent edges
2. tiles with mirrored edges
3. tiles with matted edges (LHCb like)

The results are presented in Figure 11A, averaging over narrow (1mm wide) bands precisely in between the fiber rows. Tiles with transparent edges have the lowest and most non-uniform light collection efficiency. Mirroring of the tile edges allows to increase the light yield by a factor of 3 and improves the uniformity, but does not compensate dead material effects. Chemical treatment of tile edges resulting in a diffuse reflection of the scintillating light allows a factor of 2 increase of overall light yield and compensates the decrease in detector response on the outer borders of the calorimeter modules due to dead material. This could be compared with experimental tests of the light yield in transparent and matted tiles shown in Figure 11B. The predictions of the ray-tracing program are fully supported by the experimental data.

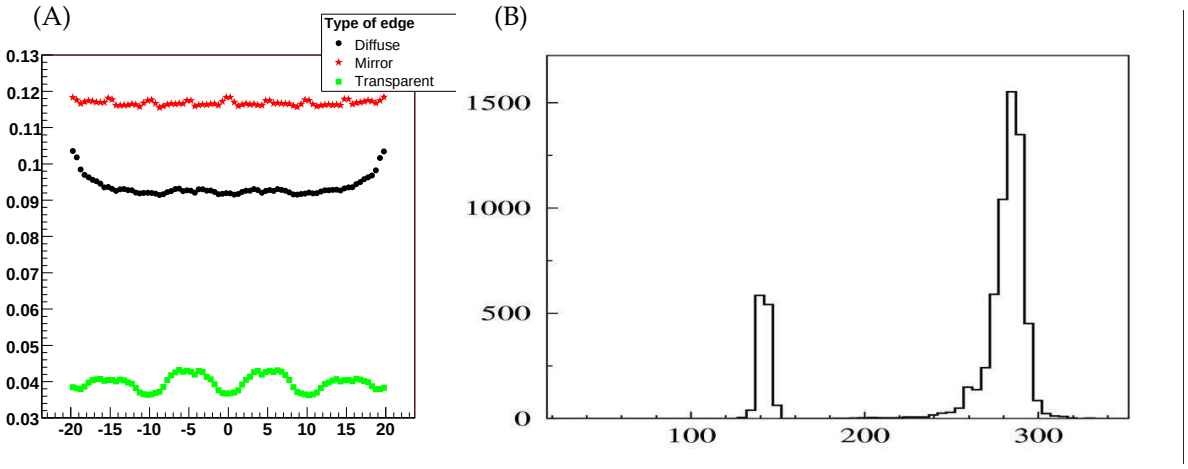

Figure 11 (A) Light collection efficiency simulated for transparent (squares), mirrored (stars) and matted (solid dots) tiles; (B) Experimental measurements of overall light yield in the scintillator tiles. The left and right peaks correspond to the transparent and matted tiles, respectively.

We have also calculated the overall light yield for the three types of plastic tiles used in the outer, middle and inner sections of the LHCb ECAL. The results of this simulation were compared with the experimental measurements of the light yield performed at the test beam and at a dedicated test bench using cosmic particles [9], as shown in Table 1. The ray-tracing program was not tuned to reproduce the absolute value of the light yield; therefore we have used the inner module simulation results for normalization of the experimental data. The simulation results agree with the experimental data within 6%.

4 Light collection uniformity

On average only a few percent of scintillating light is captured by the WLS fibers, re-emitted in forward (backward) direction and finally registered by the photo detectors. A considerable fraction (25-50%) of this light is delivered to the PMT by WLS fibers surrounding the photon production point.

The exact share of such direct light capture varies with the distance to the WLS fiber and is responsible for the so-called local or inter-fiber light collection non-uniformity. The remaining light is propagating inside the plastic tile, crossing it several times and finally being captured by a WLS fiber with a certain probability. The probability of non-direct light capture is slightly higher in the tile center. On top of that, the probability of non-direct light capture usually decreases at the tile edges because of higher light absorption there. These two effects are responsible for the so-called global light collection non-uniformity. The drop of light collection at the tile edges is strongly enhanced with energy losses in the stainless steel (and paper) - a dead material which is not sampled by the scintillator. The maximal difference in light collection efficiency could be as much as 18% over the 4mm thick plastic tile. This is obviously a non negligible effect which should be understood, minimized and taken into account in the reconstruction algorithms. The technology of the tile edges matting helps to improve the situation as shown in Figure 12 for the light collection efficiency calculated for a plastic tile of the inner type calorimeter module. Non-direct light capture (shown with solid dots) does not drop at the tile edges anymore; it even increases there, compensating the effect of dead material as was discussed in the previous chapter. A small decrease in the curve of non-direct light capture near the fibers is explained with ”screening” effects. The fiber holes ”screen” photons that have been produced nearby these remote fiber holes.

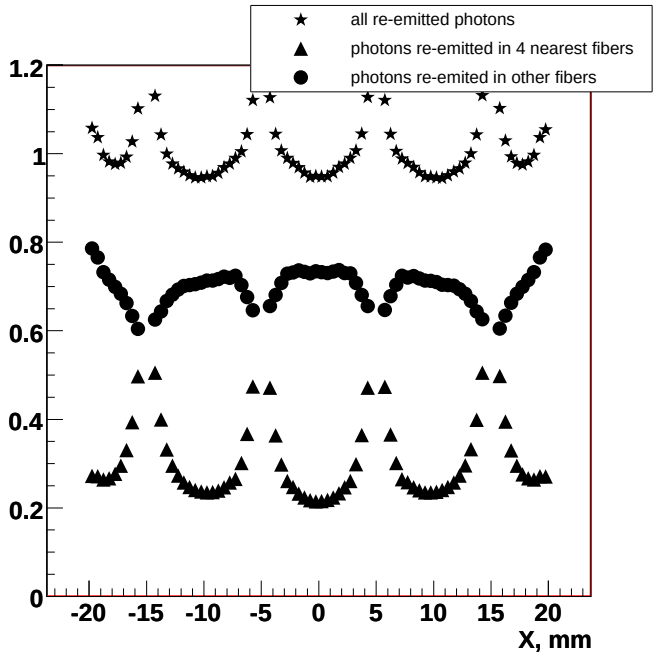

Figure 12 Light collection efficiency simulated in a plastic tile from the inner section of the LHCb ECAL. The results are presented for a narrow band scanning over the fiber positions. The net efficiency (stars) is a sum of direct light capture (triangles) and non-direct light capture (solid dots).

The net light collection efficiency as a function of the photon production coordinates in the plastic tile is has a rather complicated dependence and could hardly be approximated with a simple formula. It was studied with a dedicated Monte Carlo program simulating all stages of the light propagation and absorption in the plastic tiles. The program parameters were tuned with experimental data collected during several beam test periods for all three types of the LHCb ECAL modules, and one special module build with extremely thin (0.5 mm) plastic and lead absorber plates. High statistical samples of 100 GeV/c muons were used to scan the surface of the modules *with 1 mm steps*. Experimental results obtained for the inner calorimeter cell are presented in Figure 13 for two 1 mm wide bands — scanning over a fiber row (right plot) and scanning between two fiber rows (left plot). The hatched histogram shows the predictions of GEANT package convoluted with the effective 2D light collection efficiency maps from our dedicated simulations. The global non-uniformity is negligible. The special chemical treatment of the tile edges increased the light collection efficiency, compensating effects of dead material between the modules.

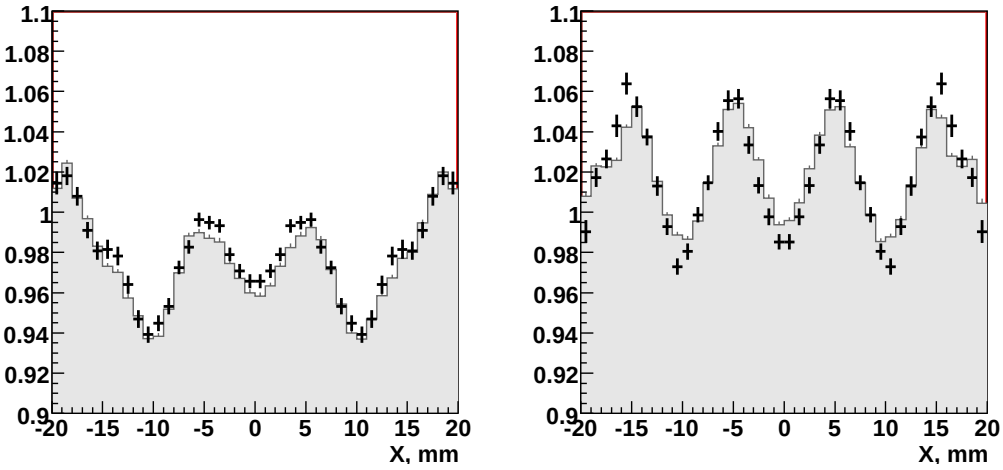

Figure 13 Response uniformity of the inner LHCb module measured with muons (error bars) and simulated (hatched histogram). The scan was made in 1 mm wide bands between two fiber rows (left) and through the fiber positions (right).

An 18% (min to max) inter-fiber variation in light collection uniformity, as seen in the top curve of Figure 12, is translated into ∼9% variation of the calorimeter response to MIP particles, which is smeared with 200 μm spatial resolution of the beam test tracking system, δ-electrons depositing energy far from the track impact point, and multiple scattering in the calorimeter stack material. Results for the middle calorimeter module are very similar. In the outer modules the inter-fiber distance is significantly higher (15 mm instead of 10 mm in the other modules), which is the reason of in increased local light collection non-uniformity up to 28%. Corresponding experimental results for the outer calorimeter module are presented in Figure 14 together with GEANT simulation predictions. The visible variation of the MIP particle response is diluted by a worse spatial resolution of the tracking system used for those tests. An increased inter-fiber distance smoothes the behavior of light collection efficiency between the fibers.

Electromagnetic showers are much wider in comparison with almost point-like energy depositions of

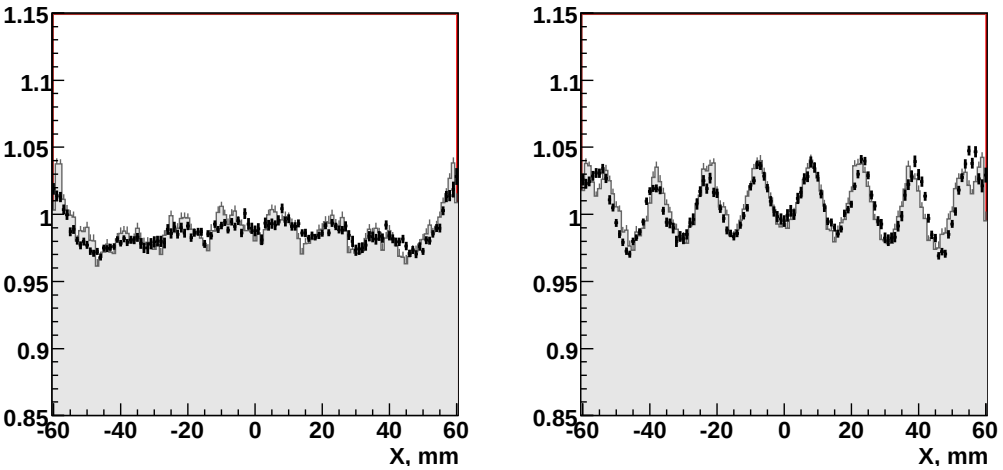

Figure 14 Response uniformity of the outer LHCb module measured with muons (error bars) and simulated (hatched histogram). The scan was made in 2 mm wide bands between two fiber rows (left) and through the fiber positions (right).

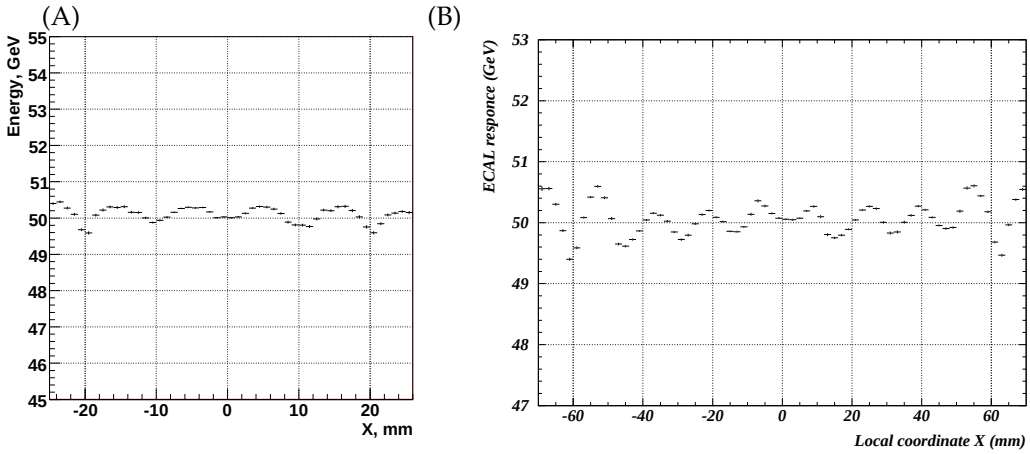

Figure 15 Response uniformity of the inner (left) and outer (right) calorimeter modules measured with 50 GeV/c^2 electrons. The scan was made in 10 mm wide bands through the fibre positions.

minimum ionizing particles. Therefore the variations of reconstructed energy for electrons and photons are considerably reduced as compared to muons. The results of a lateral scan of the inner and outer ECAL modules with 50 GeV/c^2 electrons are shown in Figure 15 for 10 mm wide bands scanning through the WLS fibre positions. In the cell of the inner module we observed a $\pm 0.5\%$ variation of response (left plot). This cell is located in the center of the module and therefore the effects of dead material in the module periphery are not seen. These effects were studied with an outer ECAL module (right plot) where we observed a $\pm 1.3\%$ variation of response. The increase of non-uniformity is caused by higher inter-fibre distances in this type of module. The most significant variations are seen at $\pm 60mm$ from the module center, corresponding to the transition from one module to another, which is filled with a 100 μm steel tape. The energy losses in the dead material (steel tapes) are overcompensated. The increase of light collection efficiency at the tile edges is most clearly seen for bands in between two fibre rows. The comparison of experimental data with MC simulation for this band is shown in Figure 16 for the inner ECAL module. The Monte Carlo perfectly describes the experimental measurements. The variation of the ECAL response to electrons and photons in the LHCb detector will be significantly decreased due to the nonzero impact angles.

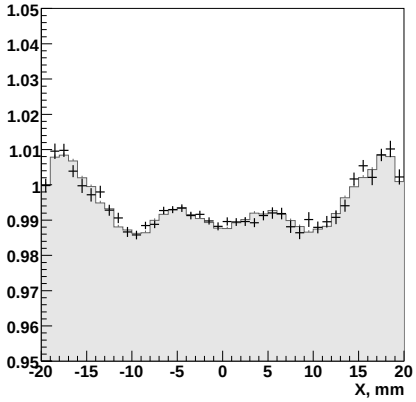

Figure 16 Response uniformity of inner LHCb calorimeter module measured with 50 GeV/c^2(error bars) compared with simulation results (hatched histogram). The scan was made in 1 mm wide bands between two fiber rows. The average response of the module for experimental data and MC simulation was normalized to unity.

5 Energy resolution

The energy resolution of the LHCb ECAL modules was studied at the test beam. We used the following standard parametrization:

$$\frac{dE}{E} = \frac{\boldsymbol{a}}{\sqrt{E}} \oplus \boldsymbol{b} \oplus \frac{\boldsymbol{c}}{E} \text{ (E in GeV)}$$

, where $\boldsymbol{a}$, $\boldsymbol{b}$ and $\boldsymbol{c}$ stand for the stochastic, constant and noise terms, respectively. Depending on the module type and experimental conditions the stochastic and constant terms were measured to be $8.5\% < a < 9.5\%$ and b about 0.8%. The noise term obtained from the fit agrees well with the measurement of pedestal widths. For the inner module we have compared the "local" energy resolution obtained for particles hitting a small ($2 \times 2\ mm^2$) area of calorimeter cell with the energy resolution averaged over almost the whole cell ($30 \times 60\ mm^2$). The result of the combined fit is presented in Figure 17. It illustrates the net influence of the light collection non-uniformity on the energy resolution. Parameter P1 stands for the stochastic term, which is forced to be the same in both cases (left and right plots). Parameter P4 represents the electronics noise (in MeV). Parameters P2 and P3 stand for the constant term of the energy resolution obtained for large (0.83%) and small (0.47%) cell areas, respectively.

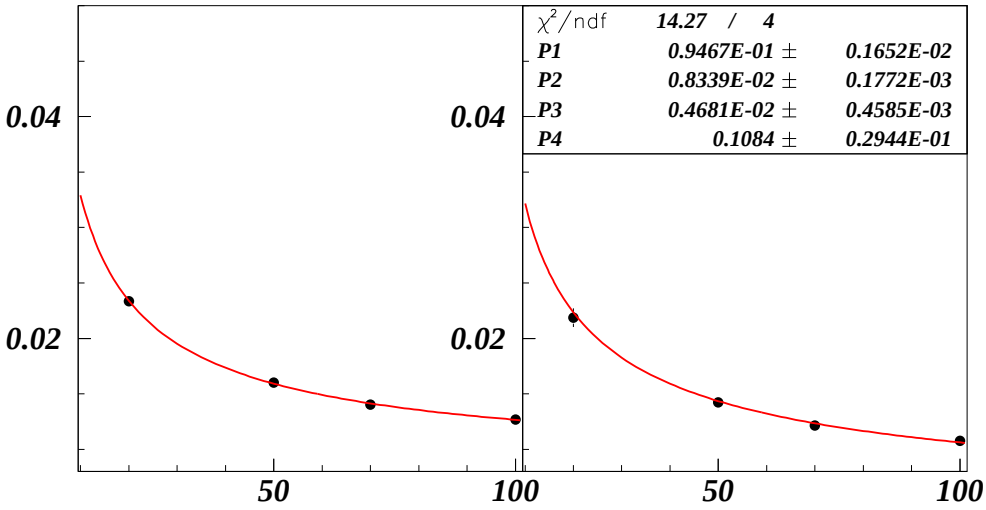

Figure 17 Combined fit of energy resolution in the inner module of the LHCb ECAL. Data shown in the left plot were collected over a large ($30 \times 60\ mm^2$) area of the calorimeter cell and are affected by non-uniformity of the light collection. Data for the right plot were collected in a small ($2 \times 2\ mm^2$) region of the calorimeter cell.

6 Conclusions

The light collection efficiency of the LHCb ECAL modules was studied at the test beam with energetic muons and electrons. In order to verify our understanding of the ECAL behavior we have developed a dedicated Monte Carlo program to simulate the light propagation in different scintillator tiles. Parameters of this program were tuned using experimental data collected during beam tests. This Monte Carlo simulation is able to reproduce all measured effects.

The monitoring system has proven to be an invaluable tool for our systematic study of the LHCb electromagnetic calorimeter properties at the test beam facility. The system completely satisfies our demands on stability for the methodical tests of the LHCb ECAL modules. It allows us to perform measurements with an accuracy of $\pm 0.2\%$ over two weeks without any temperature stabilization.

Acknowledgements

We would like to thank the CERN-SPS machine crew for the operation of the beam. We are indebted to L.Gatignon for his work and organization for data taking in the SPS-X7 beam line. We are also grateful to R. Lindner, N. Neufeld and C. Gaspar from CERN LHCb team for their help in test beam measurements organization. Many thanks we address to J. Lefrancois for his useful advices.

7 References

[1] A. Bazilevsky *et al.*, IEEE Transactions on Nuclear Science v.43, No. 3 (1996)

[2] A. Maio *et al.*, "STIC, The New DELPHI Luminosity monitor", in Proceeding of the IV International Conference on Calorimetry in High Energy Physics, p.165, Isola d'Elba, Italy, September 19-25, 1993

[3] HERA-B Collaboration, HERA-B Design Report, DESY-PRC 95/01 January 1995

[4] LHCb Calorimeters, Technical Design Report, CERN/LHCC/2000-0036

[5] L. Gatignon, "The West experimental Area at the CERN SPS", CERN-SL-2000-016-EA

[6] J. Spanggaard, "Delay Wire Chambers — a user guide", CERN-SL-98-023-BI

[7] M. Born and E. Wolf, "Principles of Optics", 1980 6^{th} ed., Pergamon Press

[8] CERN Program Library Long Writeup W5013 (1993)

[9] A. Aref'ev *et al.*, "Design, construction, quality control and performance study with cosmic rays of modules for the LHCb electromagnetic calorimeter", LHCb-2007-148